Hindawi Publishing Corporation
Advances in OptoElectronics
Volume 2011, Article ID 432803, 11 pages
doi:10.1155/2011/432803

Research Article

High Molar Extinction Coefficient Ru(II)-Mixed Ligand Polypyridyl Complexes for Dye Sensitized Solar Cell Application

Malapaka Chandrasekharam,[1] Ganugula Rajkumar,[2] Chikkam Srinivasa Rao,[1] Thogiti Suresh,[1] Yarasi Soujanya,[3] and Paidi Yella Reddy[2]

[1] *Inorganic and Physical Chemistry Division, Indian Institute of Chemical Technology, Uppal Road, Tarnaka, Hyderabad 500 607, India*
[2] *Aisin Cosmos R&D Co. Ltd, Indian Institute of Chemical Technology, Uppal Road, Tarnaka, Hyderabad 500 607, India*
[3] *Molecular Modelling Group, Indian Institute of Chemical Technology, Uppal Road, Tarnaka, Hyderabad 500 607, India*

Correspondence should be addressed to Malapaka Chandrasekharam, csmalapaka@yahoo.com

Received 21 April 2011; Accepted 7 June 2011

Academic Editor: Surya Prakash Singh

Two new ruthenium(II) mixed ligand terpyridine complexes, "Ru(Htcterpy)(NCS)(**L1**) ($N(C_4H_9)_4$), m**LBD1**" and Ru(Htcterpy)(NCS)(**L2**)($N(C_4H_9)_4$), m**LBD2** were synthesized and fully characterized by UV-Vis, emission, cyclic voltammogram, and other spectroscopic means, and the structures of the compounds are confirmed by ^{1}H-NMR, ESI-MASS, and FT-IR spectroscopes. The influence of the substitution of **L1** and **L2** on solar-to-electrical energy conversion efficiency (η) of dye-sensitized solar cells (DSSCs) was evaluated relative to reference black dye. The dyes showed molar extinction coefficients of 17600 M^{-1} cm^{-1} for m**LBD1** and 21300 M^{-1} cm^{-1} for m**LBD2** both at λ maximum of 512 nm, while black dye has shown 8660 M^{-1} cm^{-1} at λ maximum of 615 nm. The monochromatic incident photon-to-collected electron conversion efficiencies of 60.71% and 75.89% were obtained for m**LBD1** and m**LBD2** dyes, respectively. The energy conversion efficiencies of m**LBD1** and m**LBD2** dyes are 3.15% (J_{SC} = 11.86 mA/cm^2, V_{OC} = 613 mV, ff = 0.4337) and 3.36% (J_{SC} = 12.71 mA/cm^2, V_{OC} = 655 mV, ff = 0.4042), respectively, measured at the AM1.5G conditions, the reference black dye-sensitized solar cell, fabricated and evaluated under identical conditions exhibited η-value of 2.69% (J_{SC} = 10.95 mA/cm^2, V_{OC} = 655 mV, ff = 0.3750).

1. Introduction

Among various photo voltaic technologies, dye-sensitized solar cells (DSSCs) are known to be less expensive, easy to fabricate and very efficient at varied incident angle of light. Therefore, intense attention has been devoted in the last two decades to the synthesis of new materials as sensitizers, metal oxide semiconductors, counter electrode materials, electrolytes, and so forth, for applications in high-performance and long durable DSSCs [1–6]. Especially sensitizer plays important role in the DSSCs device for obtaining high-efficiency and long-term durability because of the possibility to chemically modify the sensitizer for better anchoring on TiO_2, electron injection property and HOMO-LUMO tuning. To achieve this, many researchers around the world have been working either on modification of various reported sensitizers or designing new sensitizers. A variety of ruthenium(II) polypyridyl, terpyridyl and tetrapyridyl complexes, metal-free organic sensitizers, porphyrins, and phthalocyanines have been developed, since Graetzel introduced the first efficient nanocrystalline TiO_2 solar cell sensitized with *cis*-bis(thiocyanato) bis(2,2′-bipyridyl-4,4′-dicarboxylato) ruthenium(II) bis (tetrabutylammonium) (**N**719) [7–14]. Introduced in 1997, another ruthenium complex, black dye [tri(isothiocyanato)-2,2′,2″-terpyridyl-4,4′,4″-tricarboxylate ruthenium(II)] showed broad spectral absorption (ranging from 400 to 800 nm) and achieved a record 10.4% (air mass1.5) solar to power conversion efficiency in full sunlight [15, 16]. However, the molar extinction coefficient of the sensitizer is relatively much lower as compared to the most efficient **N**719 dye. In addition, long-term durability is found to be one of the key limitations of

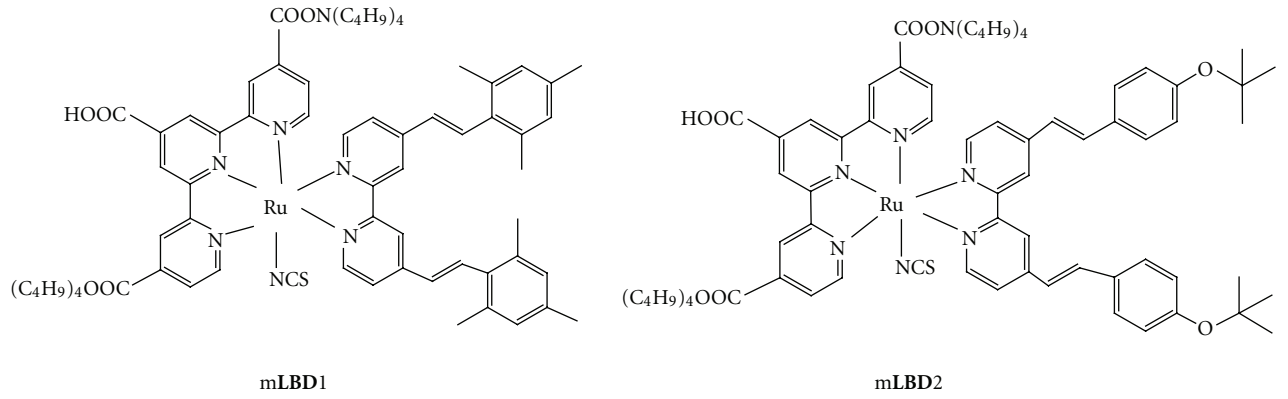

m**LBD**1 m**LBD**2

Figure 1: Structures of m**LBD** dyes.

the black dye-sensitized solar cell preventing them from their applicability in outdoor applications. The photodegradation of the dye anchored on TiO_2 resulting from the interactions of the three NCS anions are proposed as the reasons for less stability. Sensitizers **HRD**2 [17] and **K**77 [18, 19] have been reported wherein 4,4′-bis(2,4,6-trimethylstyryl)-2,2′-bipyridine (**L**1) and 4,4′-bis(4-*tert*-butoxystyryl)-2,2′-bipyridine (**L**2) serve as ancillary ligands respectively, and substantially increased molar extinction coefficient (ε) along with improved solar-to-electrical energy conversion efficiencies (η) were obtained in DSSC devices. As a part of our ongoing program on synthesis of new materials and their photovoltaic performance evaluation in DSSC devices [8, 17, 20–24], we envisaged that the design of new sensitizers with increased molar extinction coefficient, long-term durability, combined with broad absorption can be realized by substituting two thiocyanate anions of the black dye with electron donating conjugated bipyridine ligands. Thus, the terpyridine tricarboxylic acid strongly anchors on the semiconductor TiO_2 surface, while the bipyridine ligands with strong electron donating groups bring about the unidirectional electron flow for efficient electron injection. With this new mixed ligand ruthenium complex concept, we report in this paper the synthesis and characterization of two new terpyridine and bipyridine-based ruthenium(II) complexes "Ru(Htcterpy)(NCS)(**L**1) ($N(C_4H_9)_4$), m**LBD**1" and Ru(Htcterpy)(NCS)(**L**2)($N(C_4H_9)_4$), m**LBD2**, (Figure 1). Further the photovoltaic properties of test cell DSSCs constructed from these sensitizers and black dye are functionally evaluated and the influence of **L**1 and **L**2 on solar-to-electricity energy conversion efficiency (η) were studied under similar fabrication and evaluation conditions.

2. DSSC Device Fabrication

The fluorine-doped SnO_2 (FTO) conducting glass plates (Nippon Sheet Glass, 4 mm thick, 8 Ω/sq) were cleaned with a detergent solution, rinsed with water and ethanol to remove organics or any other contaminants, and then dried. The glass plates were treated in a UV-O_3 system for 20 minutes and then laid a compact layer by treating the plates with 40 mM $TiCl_4$ aqueous solution and heating at 70°C for 30 minutes to facilitate a good mechanical contact between the nanocrystalline TiO_2 and the conducting FTO matrix. Over the glass plate, 9 μm thickness D18T (18 nm TiO_2 particles) was laid as transparent layer and then a 4.8 μm thickness HPW-400 (400 nm anatase TiO_2 particles) was laid as scattering layer successively one over the other. The electrodes were coated with the TiO_2 pastes, thus have an active area of 0.74 cm^2, and were heated gradually under an air flow for 5 minutes each at 325°C and 375°C and for 15 minutes each at 450°C and 500°C. The TiO_2 electrodes were then allowed to cool and when the temperature attained to around 100°C, immersed in dye solutions of ethanol and remained soaked for 16 hours under dark. After taking out from the dye solutions, the electrodes were rinsed with ethanol to remove the unadsorbed dye molecules and then dried under nitrogen gas. The counter electrodes were prepared by treatment of FTO glass plates (TEC 15, 2.2 mm thickness, Libbey-Owens-Ford Industries) with $TiCl_4$ and further with a drop of H_2PtCl_6 solution (2 mg of Pt in 1 mL of ethanol) and heated at 430°C for 15 minutes. The dye sensitized TiO_2 electrode and Pt counter electrode were assembled into a sealed sandwich type cell by heating with a hot-melt surlyn film (Surlyn 1702, 25 μm thickness, Du-Pont) as a spacer in-between the electrodes. The ionic liquid electrolyte was filled through the predrilled hole present on the counter electrode using vacuum filling technique, the hole was sealed with a Surlyn disk and a thin glass to avoid leakage of the electrolyte.

3. Results and Discussion

3.1. Synthesis. The synthesis of these complexes is achieved following Scheme 1. The oxidation of 4,4′4″-triethyl-2,2′:6′2″-terpyridine to the tricarboxylic acid followed by esterification gives 4,4′,4″-trimethoxycarbonyl-2,2′:6′2″-terpyridine. The bipyridyl ligands **L**1 and **L**2 were synthesized by condensing 2,4,6-trimethylbenzaldehyde or 4-*tert*-butoxybenzaldehyde with tetraethyl 2,2′-bipyridine-4,4′-diylbis(methylene)diphosphonate under Wittig conditions. The reaction of ruthenium trichloride with the triester in presence of EtOH/$CHCl_3$ under reflux for 4 hrs results in the trichloro Ru-complex. The complex is further refluxed for 4 hrs in DMF in presence of bipyridyl ligand (**L**1 or **L**2)

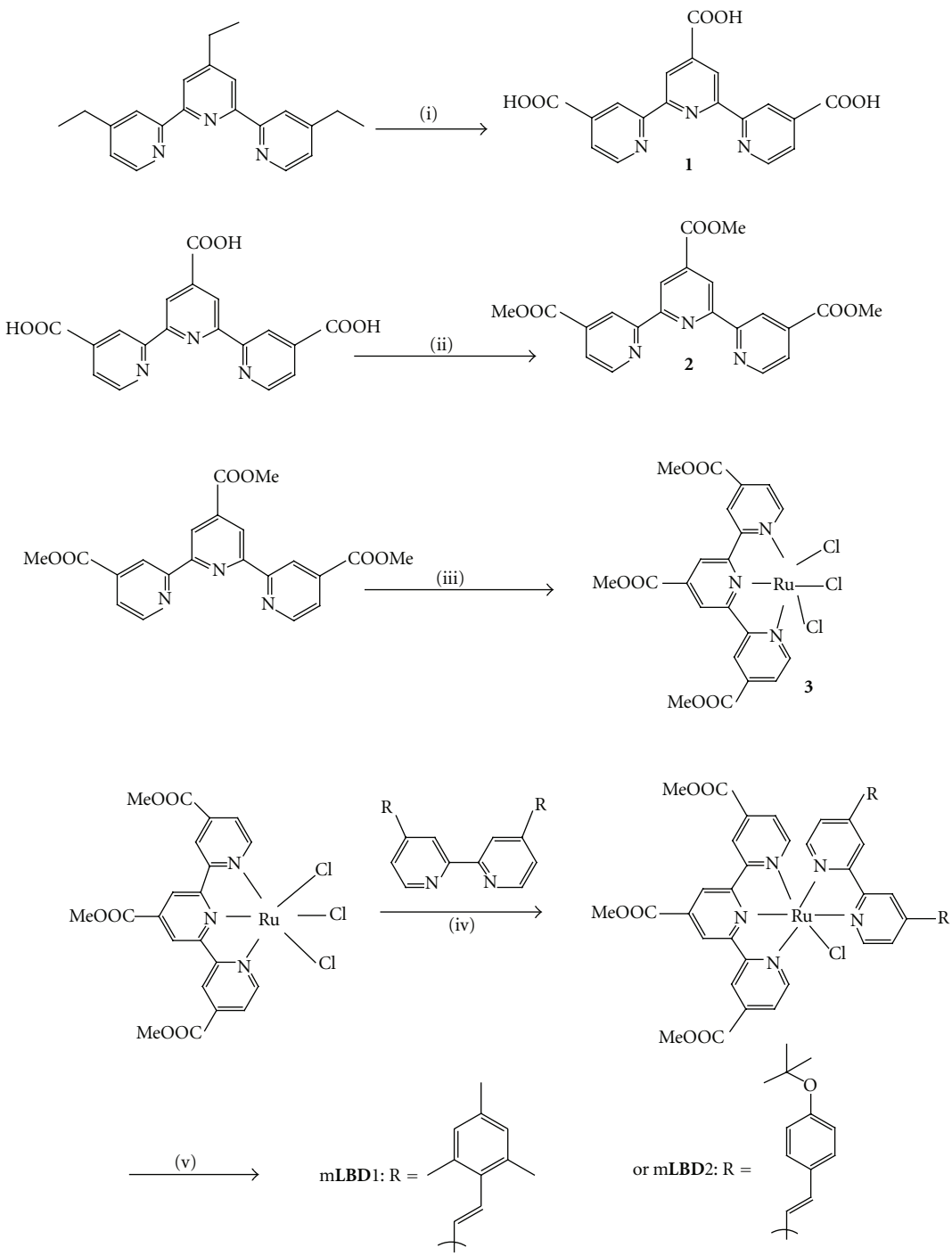

Scheme 1: Synthesis route of m**LBD** dyes; (i) $K_2Cr_2O_7$, H_2SO_4/H_2O, 80°C, 10 hours; (ii) MeOH, conc. H_2SO_4, reflux, 6 hours (iii) $RuCl_3$, $EtOH/CHCl_3$, reflux under dark, 4 hours; (iv) **L**1 or **L**2, DMF reflux, 4 hours; (v) NH_4NCS, reflux, 2 hours, TEA, water, reflux, 48 hours.

followed by addition of excess NH_4NCS, under refluxing conditions in DMF. The triester mixed ligand complex is finally treated with TEA in water under refluxing conditions for 48 hrs resulted in the formation of m**LBD1** and m**LBD**2 complexes. The crude complexes obtained were purified on Sephadex LH20 column chromatography to afford m**LBD1** and m**LBD**2 sensitizers as pure compounds. The new sensitizers were fully characterized by UV-Vis, emission, cyclic voltammogram, and other spectroscopic means, and the structures of the compounds are confirmed by ^{1}HNMR, ESI-MASS, FT-IR spectroscopes.

4,4′,4′′-triethyl-2,2′:6′2′′-terpyridine was prepared according to reported procedure ref. Tetrabutylammonium-hydroxide, 2, 4, 6-trimethylbenzaldehyde or 4-*tert*-butoxy-benzaldehyde, ammonium thiocyanate, sodiumhydride, and ruthenium trichloride were purchased from Sigma-Aldrich.

All solvents and reagents, unless otherwise stated, were of Laboratory Reagent Grade and used as received. The tetraethyl 2,2′-bipyridine-4,4′-diylbis(methylene)diphosphonate was prepared in accordance to the reported procedure. Sephadex LH-20 was procured from GE Healthcare Bio-Sciences AB, SE-75184, Uppsala and was used to purify the crude complexes on column chromatography. Brucker 300Avance ^{1}H-NMR spectrometer run at 500 MHz was employed to record the ^{1}H-NMR spectrum. Shimadzu LCMS-2010EV model with ESI probe was employed for MASS analysis. Shimadzu UV-Vis spectrometer (model 1700) and Fluorolog 3, J. Y. Horiba Fluorescence spectrometer were employed to record the electronic absorption and emission spectra.

Synthesis of 4,4′4′′-Tricarboxy-2,2′:6′2′′-Terpyridine (1). 4,4′,4′′-triethyl-2,2′:6′2′′-terpyridine (10 g, 31.55 mmol) was added to a mixture of Conc. H_2SO_4 and water (150 mL + 150 mL), and dissolved at room temperature. To this solution, $K_2Cr_2O_7$ (62.1 g, 211.4 mmol) was added in portions for about 4 hours (note: while adding $K_2Cr_2O_7$, vigorous exothermic reaction takes place, cooling is necessary to avoid the reaction temperature to exceed 50°C). The cooling bath was removed, and the reaction flask was heated to 80°C using heating mantle for 6 hours with stirring. After allowing it to cool to room temperature, the reaction mixture was poured into ice water (1200 mL). After keeping it for 4 hours at 0°C, suspension was filtered by suction. The separated greenish-yellow precipitate was washed thoroughly with distilled water (until the filtrate is colorless) and dried under vacuum. The pale yellow solid was suspended in aqueous HNO_3 (18 mL of 70%) and refluxed for 3 hours. After cooling to room temperature, the reaction mixture was poured into ice water (1000 mL) and stored at 0°C over night. The resulted white solid was collected on a sintered glass crucible (G4), washed thoroughly with water until the filtrate is colorless, and dried under vacuum to give 4,4′4′′-tricarboxy-2,2′:6′2′′-terpyridine acid, which was characterized by ^{1}H-NMR spectroscopy. ^{1}H-NMR (D_2O/NaOD) ppm: 7.72 (2H, dd), 8.22 (2H, s), and 8.62 (2H, d), 8.82 (2H, d). Chemical formula ESIMS: $C_{18}H_{11}N_3O_6$ $(M+H)^+$: 365 (100%).

Synthesis of 4,4′,4′′-Trimethoxycarbonyl-2,2′:6′2′′-Terpyridine (2). To a suspension of 4,4′4′′-tricarboxy-2,2′:6′2′′-terpyridine (20.0 g, 5.49 mmol) in absolute methanol (850 mL) was added conc. sulfuric acid (115 mL). The mixture was refluxed for 6 hours to obtain a clear solution and then cooled to room temperature. Water (400 mL) was added and the excess methanol removed under vacuum. The pH was adjusted to neutral with NaOH solution, and the resulting precipitate was filtered and washed with water (pH = 7.0). The solid was dried to obtain 17.0 g of desired compound. ^{1}H-NMR (300 MHz, $CDCl_3$, δ): 3.95 (3H, s, CH_3); 4.05 (6H, s, CH_3); 7.98 (2H, d, J = 6 Hz, aryl H on C5 and C5′); 8.88 (2H, d, J = 6 Hz, aryl H on C6 and C6′); 9.00 (2H, s, aryl H on C3 and C3′); 9.20 (2H, d, J = 6 Hz) ESIMS: $(C_{21}H_{17}N_3O_6)$ $(M+H)^+$: 408 (100%).

Synthesis of Ruthenium Trichloro Complex (3). Ruthenium tri chloride (642 mg, 2.5 mmol) was dissolved in a mixture of ethanol and chloroform (100 mL). To this, 4,4′,4′′-trimethoxycarbonyl-2,2′:6′2′′-terpyridine (1.0 g, 2.5 mmol) was added, and then, the reaction mixture was refluxed for 4 hours under nitrogen atmosphere in the absence of light. The progress of the reaction was monitored by UV-VIS spec-troscopy. After completion of 3 hours, the solution was concentrated on rotary evaporator. The crude trichloro compound washed with ethanol and dried under vacuum to obtain white solid (85% yield) ^{1}H-NMR (D_2O/NaOD) ppm: 8.70 (d, 2H), 8.22 (s, 2H), 8.10 (s, 2H), 7.62 (2H, d). ESIMS: $(C_{21}H_{17}Cl_3N_3O_6Ru)$ $(M+H)^+$: 615 (25%).

Synthesis of L1 and L2 (Representative Procedure). Sodium hydride (177 mg, 7.38 mmol) was washed with dry hexane (3 × 10 mL). To this suspension, a THF solution of tetraethyl 2,2′-bipyridine-4,4′-diylbis(methylene)diphosphonate derivative (560 mg, 1.23 mmol) was added, and the resulting mixture was stirred at room temperature for a period of 30 minutes. To this, 2,4,6-trimethyl benzaldehyde (546 mg, 3.69 mmol dissolved in THF) or 4-*tert*-butoxy benzaldehyde (656 mg, 3.69 mmol dissolved in THF) was added dropwise at room temperature while stirring. The reaction mixture was refluxed for 12 hours and then allowed to cool to room temperature. The reaction mixture was filtered through a short plug of silica gel using diethyl ether. The filtrate was concentrated, and methanol was added. The corresponding bipyridyl ligand was precipitated and the precipitate was filtered and washed with cool methanol. The solid was dried to obtain pure **L**1 or **L**2.

4, 4′-Bis-[2-(2,4,6-Trimethyl-Phenyl)-Vinyl]-[2, 2′]-Bipyridine(L1). ^{1}H-NMR (300 MHz, 25°C, $CDCl_3$) 2.35 (s, 18H), 6.58 (d, 1H), 6.62 (s, 4H), 7.25 (s, 2H), 7.31 (d, 1H), 8.63 (d, 2H), 8.71 (d, 2H); ESI-MS: $(C_{32}H_{32}N_2)$ $(M+H)^+$: 444 (100%).

4, 4′-Bis-[2-(2-(Tert-Butoxy Phenyl)-Vinyl)]-[2, 2′]-Bipyridine(L2). ^{1}H-NMR (200 MHz, 25°C, $CDCl_3$)*d* [ppm]: 8.67 (d, 2H), 8.54 (s, 1H), 7.46 (m, 8H), 7.06 (m, 6H), 1.40 (s, 18H). Chemical formula $(C_{34}H_{36}N_2O_2)$, ESI-MS: Calcd for $(M+H)^+$: 504 (55%).

*Synthesis of m**LBD** Complex (Representative Procedure).* Dry DMF (100 mL) was placed into 250 mL RB flask, to which ruthenium trichloro complex (200 mg, 0.32 mmol) was added under nitrogen atmosphere, the resulting solution was stirred for five minutes, and then, **L**1 or **L**2 (0.391 mmol) was added. The reaction mixture was refluxed for 4 hours under N_2 atmosphere. After completion of 4 hours, the mixture was cooled to 80°C, and then, aqueous solution of ammonium thiocyanate (768 mg in 2 mL of water) was added. The mixture was further refluxed for 2 hours. The progress of the reaction was monitored by UV-VIS spectroscopy. After 2 hours, the reaction mixture was cooled to room temperature, and triethylamine was added followed by water (2 mL + 2 mL). The mixture was further refluxed for 48 hours. Then,

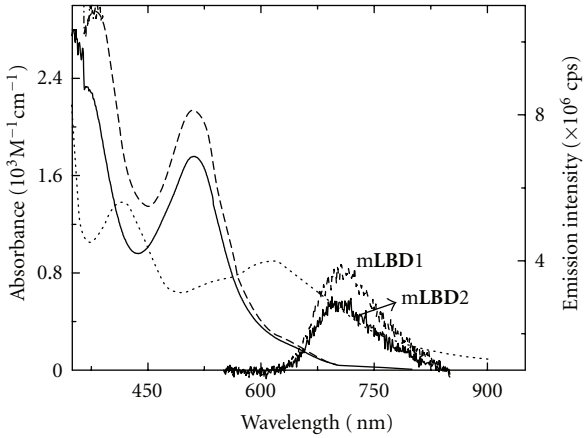

FIGURE 2: Equimolar absorption spectra of m**LBD**1 (—), m**LBD**2 (- - -) and black dye (...) in ethanol and emission spectra of m**LBD**1and m**LBD**2.

the solvent was removed on rotary evaporator, and water was added to get the precipitate. The solid was filtered, washed with water and dried under vacuum. The crude compound was dissolved in MeOH and methanolic TBA and purified on Sephadex LH-20 column chromatography eluting with MeOH. The main band was collected and concentrated. This purification procedure was repeated 3-4 times to afford m**LBD**1 and m**LBD**2 dyes in the pure form.

mLBD1. ^{1}H-NMR (300 MHz, CD_3OD + $CDCl_3$, δ_H): 9.50 (d, 1H), 8.95 (s, 2H), 8.88 (d, 1H), 8.75 (s, 2H), 8.60 (s, 1H), 8.05 (d, 1H), 7.85 (d, 2H), 7.75 (m, 4H), 7.40 (d, 2H), 7.10 (d, 1H), 6.90 (s, 1H), 6.85 (s, 2H), 6.75 (s, 2H), 6.40 (d, 1H), 3.50–0.86 (m, 90H); ESI-MASS: $RuC_{51}H_{43}N_6O_6S$(1TBA)(M+) = 1211(35%). IR (KBr): ν = 2965 cm^{-1}(CH_3), 2095(NCS), 1605(COO^-_{asym}), 1529(BPy), 1474(BPy), 1354(COO^-_{sym}).

mLBD2. ^{1}H-NMR (300 MHz, CD_3OD + $CDCl_3$, δ_H): 9.65 (d, 1H), 9.10 (s, 2H), 9.00 (s, 1H), 8.90 (s, 2H), 8.70 (s, 1H), 8.20 (d, 1H), 7.85 (d, 2H), 7.75–7.38 (m, 10H), 7.25–6.75 (m, 6H), 3.50–0.86 (m, 90H). ESI-MASS: $RuC_{53}H_{47}N_6O_8S$(1TBA)(M + 1) = 1272(80%). IR (KBr): ν = 2965 cm^{-1}(*t*-butyl), 2095(NCS), 1605(COO^-_{asym}), 1529 (BPy), 1474(BPy), 1354(COO^-_{sym}).

3.2. Absorption, Emission, and Electrochemical Properties. To have a preliminary evaluation of the light harvesting capacity of the new sensitizers, the electronic absorption spectra were recorded in ethanol and compared with that of black dye. As compared to black dye, these new sensitizers show intense UV absorption band at around 380 nm, which are assigned to the ligand centred π-π^* transition of the H3tctpy ligand [25, 26] and other intense low-energy absorption band at around 510 nm. The low-energy absorption band is assigned to metal-to-ligand charge-transfer (MLCT) transition. Absorption spectra of these dyes are very different from that of black-dye, which exhibit intense and broad absorption bands at about 430 and 520 nm and a distinct shoulder low-energy absorption band at around 700 nm extending up to 850 nm (Figure 2). As compared to black dye, the low-energy absorption bands of m**LBD** dyes are blue-shifted. The dyes showed molar extinction coefficients of 17600 M^{-1} cm^{-1} for m**LBD**1 and 21300 M^{-1} cm^{-1} for m**LBD**2 both at λ maximum of 512 nm, while black dye has shown 8660 M^{-1} cm^{-1} at λ maximum of 615 nm. The m**LBD** dyes increased the light-harvesting ability of the new sensitizers by enhancing their molar extinction coefficients by around 50%, especially in the wavelength region of 400–550 nm, which could be the contribution of extended π-conjugation of these bipyridyl ligands **L**1 and **L**2.

In case of m**LBD** dyes, the increased molar extinction coefficient is expected due to extension of π-conjugation, which is akin to the molecular cosensitization for efficient panchromatic DSSC sensitisers [27]. What is expected of these dyes is maintaining the absorption spectrum of black-dye, while enhancing the molar extinction coefficient. But the introduction of these bipyridyl ligands shifted the absorption spectrum towards blue region. To understand the molar extinction coefficient's augment and the blue-shifted absorption spectrum, time-dependent density functional theory calculations were run based on DFT optimized structure in ethanol medium. The conductor-like polarizable continuum model (C-PCM), which accounts for the effects of the solvent molecule ethanol was used along with the calculations. In m**LBD** dyes, the replacement of two thiocyanato anions by a single chelating π-conjugated bipyridine ligand stabilizes the ground state with less electron donation to the centre ruthenium(II), and this causes a decrease in the overall energy of the t2g metal orbitals. For these complexes, the low-energy MLCT transition bands from this orbital to LUMO exhibit significant blue shift [28].

Besides the molar extinction coefficient, the photovoltaic performance of DSSC is also influenced by quantity of absorbed dye and its pattern over TiO_2 surface, which is further dependent on the size and geometrical structure of photosensitizer. To investigate further, the absorption measurements over TiO_2 films were carried out by staining 7 μm thick TiO_2 electrodes in 0.3 mM dye solutions prepared in ethanol for 16 hours under the dark. After that the electrodes were washed with ethanol to remove unadsorbed dye molecules and dried under nitrogen purging. The absorptions recorded using UV-Vis spectrometer showed relatively decreased film absorptions as compared with that of black dye. The substitution of two NCS anions by 4,4′-bis(2,4,6-trimethylstyryl)-2,2′-bipyridine and 4,4′-bis(4-*tert*-butoxystyryl)-2,2′-bipyridine in the black dye increased the molecular size by more than one and half times, and additionally, this influenced the packing densities of these molecules on TiO_2 films.

Prior to fabrication of DSSCs devices, cyclic voltammetry measurements of the sensitizers were conducted to ensure that the LUMOs of these complexes are suitable for injecting electrons into the conduction band of TiO_2 and also whether their HOMOs match the energy level of the I_2/I_3^- redox couple. The cyclic voltammogram of these dyes were measured using tetrabutyl ammonium perchlorate (0.1 M in acetonitrile) as an electrolyte and ferrocene as an internal standard

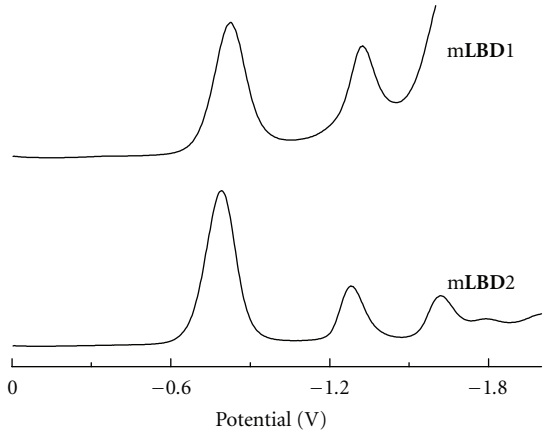

Figure 3: Differential pulse voltammograms of m**LBD** dyes, supporting electrolyte is 0.1 M tetrabutylammonium perchlorate in acetonitrile.

at 0.42 V versus SCE. Figure 3 shows the voltammogram of m**LBD** dyes in acetonitrile**.** Reversible redox were observed for these mLBD dyes, and similar to other ruthenium(II) pyridyl complexes, the measured oxidation potentials are 0.8611 and 0.8280 V, while the reduction potentials are −0.8266 and −0.7894 V versus SCE for m**LBD**1 and m**LBD**2 dyes, respectively. The more positive potentials of these sensitizers, relative to I^-/I_3^- redox couple (0.24 V versus SCE) in the electrolyte, provide a large thermodynamic driving force for the regeneration of the dyes by iodide. Based on the absorption and emission spectra of these complexes, the excitation transition energies ($E_{0\text{-}0}$) are estimated to be 1.9096 and 1.8892 eV for m**LBD**1 and m**LBD**2 dyes, respectively (obtained by converting the wavelengths of 650 nm for m**LBD**1 and 657 nm for m**LBD**2, at which their individual absorption and emission spectra (Figure 2(b)) intersect, into electron volts). The standard potentials ($\phi^0(S^+/S^*)$) calculated from the relation of $[\phi^0(S^+/S) = \phi^0(S^+/S^*) - E_{0\text{-}0}]$ are −1.0485 and −1.0612 V versus SCE for m**LBD**1 and m**LBD**2, respectively. So, $\phi^0(S^+/S^*)$ values are more negative (or higher in energy) than the conduction band edge of TiO_2 (−0.8 V versus SCE) providing ample thermodynamic driving force to inject electrons from the dye to TiO_2.

3.3. Computational Studies. In order to gain insight, the electronic ground states of fully protonated m**LBD** dyes were optimized in gaseous phase by using the density functional theory (DFT) with MPW1PW91 method and lanl2dz basis set for ruthenium and 6-31G(d) for H, C, N, O, S atoms as implemented in Gaussian 09 W and Gaussian View 5 interface software. The unoccupied and occupied frontier molecular orbitals of m**LBD** dyes are depicted in Figures 4 and 5 with isodensity surface values fixed at 0.04. The LUMO is mainly ascribed to the H3tctpy ligand with a considerable amount of p back-donation from the t2g orbitals. Moreover, the carboxylic groups show sizable contributions to LUMO and facilitate the electron injection from the excited m**LBD** dyes to the TiO_2 conduction band. Similar to other ruthenium(II) sensitizers, the HOMO has electron density distribution mainly located on the metal centre and NCS anions. TD DFT calculations showed the highly allowed transition from HOMO−2/HOMO−3 to LUMO+2 orbital, in which the electron densities of HOMO−2 and HOMO−3 are located at the metal centre, NCS ligand and the chelating **L**1 or **L**2 bipyridine, whereas that of LUMO+2 orbital is contributed to mainly by **L**1 or **L**2 bipyridine moieties. The HOMO/LUMO band gaps predicted through the DFT optimization are 2.035 and 2.045 eV for m**LBD**1 and m**LBD**2, respectively, while the band gap for parental black-dye optimized under similar conditions is 1.89 eV.

3.4. Thermal Stability. The incorporation of the ancillary bipyridine ligands into the parental black dye make the dye more hydrophobic and one of the advantages of these mixed ligand dyes could be their stability obtained by the replacement of NCS anions by stable panchromatic chelating ancillary bipyridine ligand [29]. One of the desirable parameters to retain the initial photovoltaic performance of the DSSC is the high thermal stability of the ruthenium(II) sensitizer [30], and hence, the TGA analysis of the sensitizers was performed using a TGA/SDTA 851^e thermal system (Mettler Toledo, Switzerland) at heating rate of 10°C/min in the temperature range of 25°C–600°C under N_2 atmosphere (flow rate of 30 mL/min). Film samples ranging from 8 to 10 mg were placed in the sample pan and heated, while weight losses are recorded against temperature difference. The thermograms of m**LBD** dyes are shown in Figure 6, in which the derivative of % conversion plotted against to temperature. The thermograms show a very good thermal stability (310°C for m**LBD**1 and 350°C for m**LBD**2), while under comparable conditions the black dye showed 290°C.

3.5. Photovoltaic Properties. To evaluate the influence of 4, 4′-bis(2,4,6-trimethylstyryl)-2,2′-bipyridine and 4,4′-bis(4-*tert*-butoxystyryl)-2,2′-bipyridine on the photovoltaic performance, a high-quality double-layer titania films (9 + 4.8 μm) were employed to fabricate 0.74 cm^2 active area DSSC cells in combination with a high durable electrolyte, **Z**580, containing 0.2 M I_2, 0.5 M guanidinium thiocyanate and 0.5 M N-methylbenzimidazole in a mixture of 1-propyl-3-methylimidazolium iodide/1-ethyl-3-methyl imdazolium-tetracyanoborate (65/35, v/v). Photon-to-current conversion efficiency spectrum was recorded as a function of excitation wavelength using a 300 W xenon lamp (ILC Technology, USA), which was focused through a Gemini-180 double monochromator (Jobin Yvon Ltd.). The incident photon-to-current conversion efficiencies (IPCEs) of the DSSCs constructed based on these dyes are shown in Figure 7(a). The monochromatic incident photon-to-collected electron conversion efficiencies of 60.71% and 75.89% were obtained for m**LBD**1 and m**LBD**2 dyes, respectively, over the entire visible range extending into the NIR region, which are less than unity suggesting a low-charge collection yields. The photo current-voltage measurements were executed under air mass (AM) of 1.5 sunlight and the resultant *I-V* curves are shown in Figure 7(b). The photovoltaic parameters of m**LBD** dyes are compared with that of black dye-sensitized solar

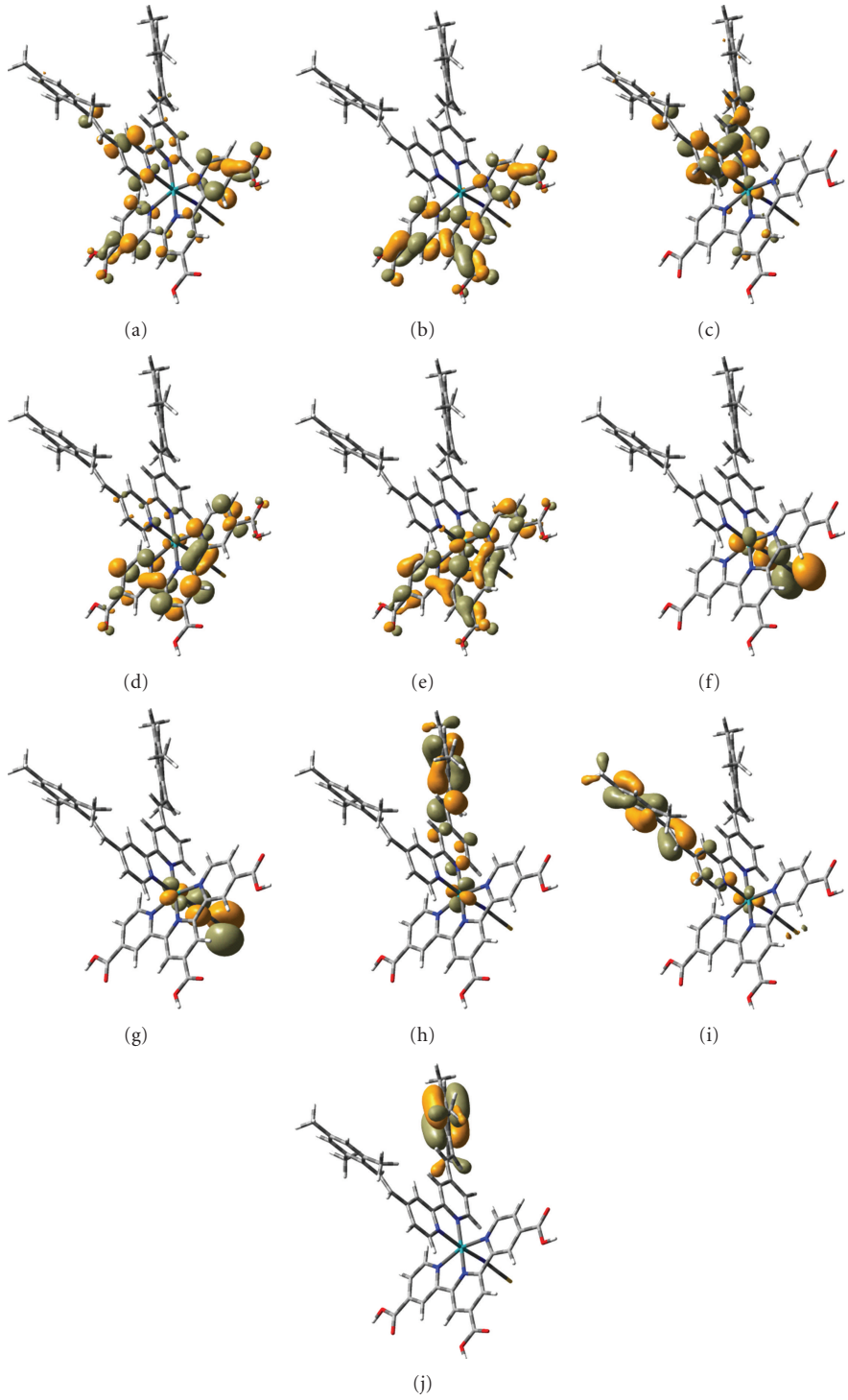

Figure 4: Frontier molecular orbitals of m**LBD**1: (a) LUMO+4; (b) LUMO+3; (c) LUMO+2; (d) LUMO+1; (e) LUMO; (f) HOMO; (g) HOMO−1; (h) HOMO−2; (i) HOMO−3; (j) HOMO−4.

cell, fabricated, and evaluated under comparable conditions (Table 1).

The energy conversion efficiencies of m**LBD**1 and m**LBD**2 dyes are 3.15% (J_{SC} = 11.86 mA/cm^2, V_{OC} = 613 mV, ff = 0.4337) and 3.36% (J_{SC} = 12.71 mA/cm^2; V_{OC} = 655 mV; ff = 0.4042), respectively, under air mass of 1.5 sun light, the reference black-dye sensitized solar cell, fabricated, and evaluated under identical conditions exhibited η-value of 2.69% (J_{SC} = 10.95 mA/cm^2, V_{OC} = 655 mV, ff = 0.3750). Although the film absorptions of m**LBD** dyes over TiO_2 films are little lower as compared to that of black dye, the newly designed m**LBD** dyes were endowed with improved over

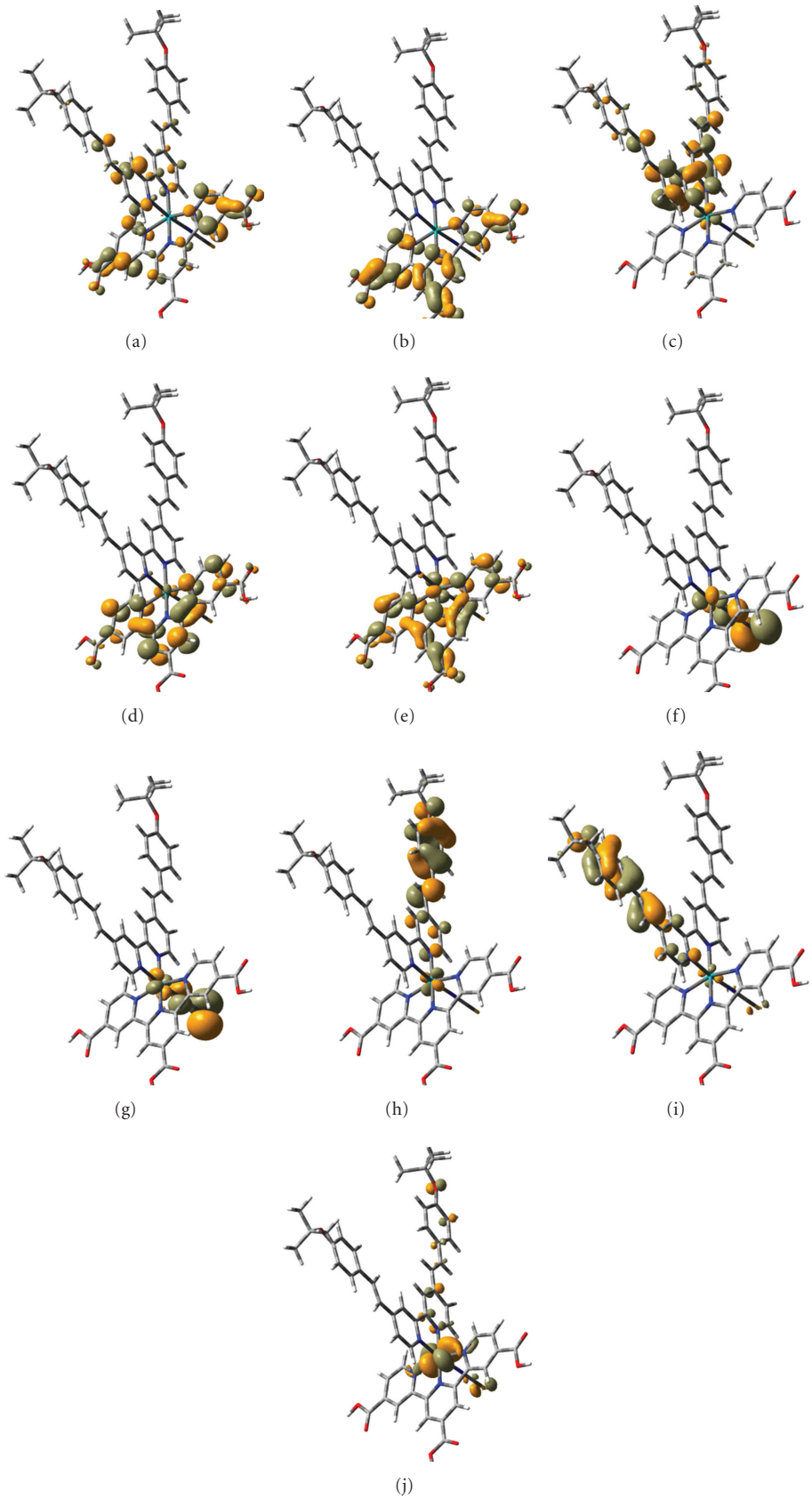

Figure 5: Frontier molecular orbitals of m**LBD**2: (a) LUMO+4; (b) LUMO+3; (c) LUMO+2; (d) LUMO+1; (e) LUMO; (f) HOMO; (g) HOMO−1; (h) HOMO−2; (i) HOMO−3; (j) HOMO−4.

Table 1: Detailed photovoltaic parameters of DSSCs.

Sensitizer	J_{SC} (mA/cm^2)	V_{OC} (mV)	ff	Efficiency (%)
m**LBD1**	11.86	613	0.4337	3.15
m**LBD2**	12.71	655	0.4042	3.36
BD	10.95	655	0.3750	2.69

Short-circuit photocurrent density (J_{SC}), open-circuit photovoltage (V_{OC}), fill factor (ff).

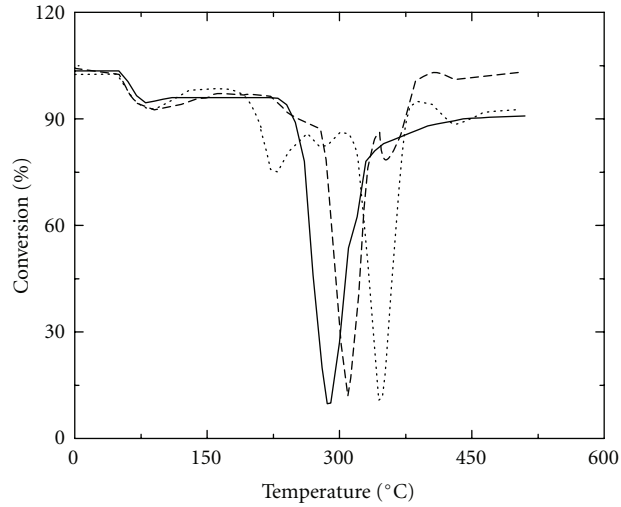

Figure 6: TG-Thermograms of m**LBD**1 (- - -), m**LBD**2 (...) and black-dye (—).

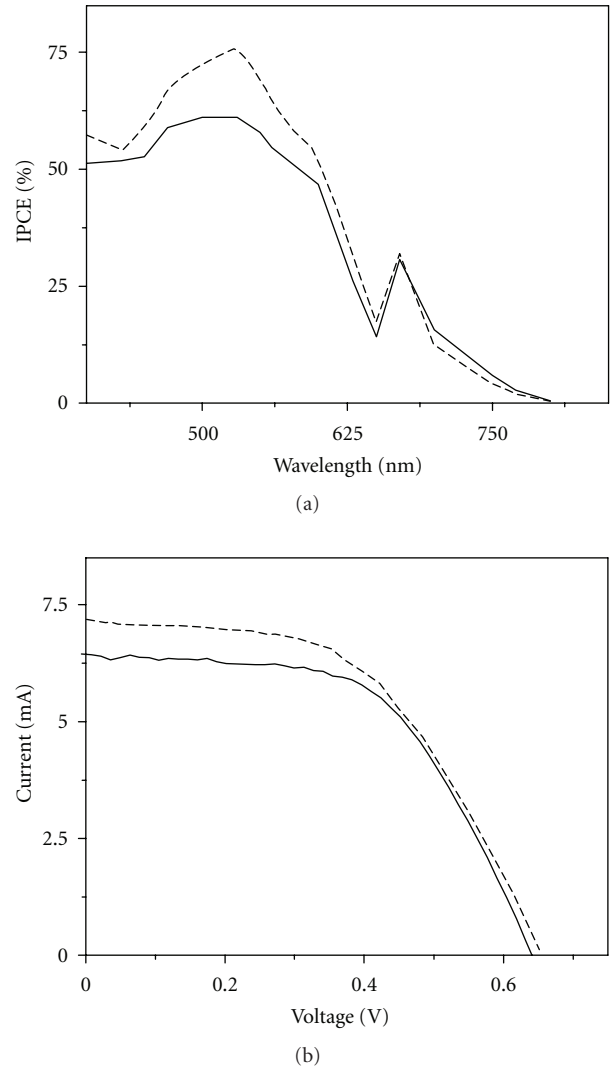

Figure 7: (a) Photocurrent action spectra of devices of m**LBD**1 (—) and m**LBD**2 (- - - -) fabricated with **Z**580 electrolyte; (b) *J-V* characteristics of m**LBD**1 (—) and m**LBD**2 (- - - -) cells (fabricated from 0.74 cm^2 active area TiO_2 electrodes), measured under an irradiance of 100 mW cm^{-2} AM1.5G sun light. Double-layer films (9.0 + 4.8 μm).

all conversion efficiencies. This could be probably due to more charge transfer to the LUMO orbitals for these dyes as compared to black dye. In the LUMO orbitals of these complexes, the electron density distributions mainly located on H_3tctpy ligand, while for black dye it is only ascribed to the centre pyridine of H_3tctpy [31]. As compared to the black dye-sensitized solar cell, the m**LBD** dyes showed higher current densities, which could be probably because of their increased incident photon to-current conversion efficiencies spectra. The m**LBD**2 sensitized solar cell gives J_{SC} = 12.71 mA/cm^2, which is slightly higher as compared to that of m**LBD**1 sensitized solar cell. Although there is no much change in their film absorptions over TiO_2 films, we presume that the increased photocurrent density and hence the efficiency of m**LBD**2 could be probably resulting from efficient dye regeneration mediated by redox electrolyte [32].

4. Conclusions

In conclusion, the new panchromatic ruthenium(II) terpyridyl-based mixed ligand dyes, m**LBD**1 and m**LBD**2 synthesized, showed much higher molar extinction coefficients at 400–550 nm remarkably with blue shift in absorption spectrum as compared to black-dye. Incorporation of conjugated light-absorbing ancillary bipyridine ligands into the new mixed ligand ruthenium(II) complexes provide a combined benefit of electron donor from ancillary conjugated bipyridyl ligand as well as electron acceptor anchoring terpyridine tricarboxylic acid in the sensitiser to achieve better charge transfer from HOMO to LUMO. Though these ancillary bipyridines do not directly interfere with active sites of TiO_2 electrode, the molecular diameter increased significantly and to some extent influenced the packing densities

of the sensitizers over TiO_2 films. These heteroleptic sensitizers exhibited better solar energy conversion efficiencies as compared to the standard black dye and m**LBD**2 sensitizer that showed an efficiency of 3.36%, highest among the three.

Acknowledgments

Ch. S. Rao thanks IICT-AIC collaborative project for a fellowship. M. Chandrasekharam thanks DST, New Delhi, for the grant of the project entitled "Advancing the efficiency and production potential of Excitonic Solar Cells (APEX)" under UK-DST consortium.

References

[1] A. Hagfeldt, G. Boschloo, L. Sun, L. Kloo, and H. Pettersson, "Dye-sensitized solar cells," *Chemical Reviews*, vol. 110, no. 11, pp. 6595–6663, 2010.

[2] D. Wei, "Dye sensitized solar cells," *International Journal of Molecular Sciences*, vol. 11, no. 3, pp. 1103–1113, 2010.

[3] M. Grätzel, "Photoelectrochemical cells," *Nature*, vol. 414, no. 6861, pp. 338–344, 2001.

[4] B. O'Regan and M. Grätzel, "A low-cost, high-efficiency solar cell based on dye-sensitized colloidal TiO_2 films," *Nature*, vol. 353, no. 6346, pp. 737–740, 1991.

[5] G. J. Meyer, "The 2010 millennium technology grand prize: dye-sensitized solar cells," *ACS Nano*, vol. 4, no. 8, pp. 4337–4343, 2010.

[6] S. M. Zakeeruddin, M. K. Nazeeruddin, R. Humphry-Baker et al., "Design, synthesis, and application of amphiphilic ruthenium polypyridyl photosensitizers in solar cells based on nanocrystalline TiO_2 films," *Langmuir*, vol. 18, no. 3, pp. 952–954, 2002.

[7] W. M. Campbell, A. K. Burrell, D. L. Officer, and K. W. Jolley, "Porphyrins as light harvesters in the dye-sensitised TiO_2 solar cell," *Coordination Chemistry Reviews*, vol. 248, no. 13-14, pp. 1363–1379, 2004.

[8] P. Y. Reddy, L. Giribabu, C. Lyness et al., "Efficient sensitization of nanocrystalline TiO_2 films by a near-IR-absorbing unsymmetrical zinc phthalocyanine," *Angewandte Chemie*, vol. 46, no. 3, pp. 373–376, 2007.

[9] D. Kuang, S. Uchida, R. Humphry-Baker, S. M. Zakeeruddin, and M. Grätzel, "Organic dye-sensitized ionic liquid based solar cells: remarkable enhancement in performance through molecular design of indoline sensitizers," *Angewandte Chemie*, vol. 47, no. 10, pp. 1923–1927, 2008.

[10] S. Tatay, S. A. Haque, B. O'Regan et al., "Kinetic competition in liquid electrolyte and solid-state cyanine dye sensitized solar cells," *Journal of Materials Chemistry*, vol. 17, no. 29, pp. 3037–3044, 2007.

[11] M. K. Nazeeruddin, F. D. Angelis, S. Fantacci et al., "Combined experimental and DFT-TDDFT computational study of photoelectrochemical cell ruthenium sensitizers," *Journal of the American Chemical Society*, vol. 127, no. 48, pp. 16835–16847, 2005.

[12] K. Hara, M. Kurashige, S. Ito et al., "Novel polyene dyes for highly efficient dye-sensitized solar cells," *Chemical Communications*, vol. 9, no. 2, pp. 252–253, 2003.

[13] M. Grätzel, "Solar energy conversion by dye-sensitized photovoltaic cells," *Inorganic Chemistry*, vol. 44, no. 20, pp. 6841–6851, 2005.

[14] C. Y. Chen, S. J. Wu, J. Y. Li, C. G. Wu, J. G. Chen, and K. C. Ho, "A new route to enhance the light-harvesting capability of ruthenium complexes for dye-sensitized solar cells," *Advanced Materials*, vol. 19, no. 22, pp. 3888–3891, 2007.

[15] M. K. Nazeeruddin, P. Péchy, T. Renouard et al., "Engineering of efficient panchromatic sensitizers for nanocrystalline TiO_2-based solar cells," *Journal of the American Chemical Society*, vol. 123, no. 8, pp. 1613–1624, 2001.

[16] Z.-S. Wang, T. Yamaguchi, H. Sugihara, and H. Arakawa, "Significant efficiency improvement of the black dye-sensitized solar cell through protonation of TiO_2 films," *Langmuir*, vol. 21, no. 10, pp. 4272–4276, 2005.

[17] L. Giribabu, C. V. Kumar, C. S. Rao et al., "High molar extinction coefficient amphiphilic ruthenium sensitizers for efficient and stable mesoscopic dye-sensitized solar cells," *Energy and Environmental Science*, vol. 2, no. 7, pp. 770–773, 2009.

[18] D. Kuang, C. Klein, S. Ito et al., "High effiiciency and stable mesoscopic dye-sensitized solar cells based on a high molar extinction cofficient Ru-sensitizer and non-volatile electrolyte," *Advanced Materials*, vol. 19, pp. 1133–1137, 2007.

[19] D. Kuang, C. Klein, Z. Zhang et al., "Stable, high-efficiency ionic-liquid-based mesoscopic dye-sensitized solar cells," *Small*, vol. 3, no. 12, pp. 2094–2102, 2007.

[20] M. Chandrasekharam, C. Srinivasarao, T. Suresh et al., "High spectral response heteroleptic ruthenium (II) complexes as sensitizers for dye sensitized solar cells," *Journal of Chemical Sciences*, vol. 123, no. 1, pp. 37–46, 2011.

[21] M. Chandrasekharam, G. Rajkumar, C. S. Rao et al., "Phenothiazine conjugated bipyridine—a new class of ancillary ligand for Ru-sensitizer in dye sensitized solar cell application," *Synthetic Metals*, vol. 161, pp. 1469–1476, 2011.

[22] M. Chandrasekharam, G. Rajkumar, C. S. Rao et al., "Polypyridyl Ru(II)-sensitizers with extended π-system enhances the performance of dye sensitized solar cells," *Synthetic Metals*, vol. 161, no. 11-12, pp. 1098–1104, 2011.

[23] M. Chandrasekharam, G. Rajkumar, C. S. Rao, P. Y. Reddy, and M. L. Kantam, "Change of dye bath for sensitisation of nanocrystalline TiO_2 films: enhances performance of dye-sensitized solar cells," *Advances in OptoElectronics*, vol. 2011, Article ID 376369, 2011.

[24] L. Giribabu, M. Chandrasekheram, M. L. Kantham et al., "Conjugated organic dyes for dye-sensitized solar cells," *Indian Journal of Chemistry A*, vol. 45, no. 3, pp. 629–634, 2006.

[25] A. Islam, F. A. Chowdhury, Y. Chiba et al., "Synthesis and characterization of new efficient tricarboxyterpyridyl (β-diketonato) ruthenium(II) sensitizers and their applications in dye-sensitized solar cells," *Chemistry of Materials*, vol. 18, no. 22, pp. 5178–5185, 2006.

[26] A. Mamo, A. Juris, G. Calogero, and S. Campagna, "Near-infrared luminescence at room temperature of two new osmium(II) terdentate polypyridine complexes," *Chemical Communications*, no. 10, pp. 1225–1226, 1996.

[27] J.-J. Cid, J.-H. Yum, S.-R. Jang et al., "Molecular cosensitization for efficient panchromatic dye-sensitized solar cells," *Angewandte Chemie International Edition*, vol. 46, no. 44, pp. 8358–8362, 2007.

[28] Y. Chi and P.-T. Chou, "Contemporary progresses on neutral, highly emissive Os(ii) and Ru(ii) complexes," *Chemical Society Reviews*, vol. 36, no. 9, pp. 1421–1431, 2007.

[29] B. S. Chen, K. Chen, Y.-H. Hong et al., "Neutral, panchromatic Ru(ii) terpyridine sensitizers bearing pyridine pyrazolate chelates with superior DSSC performance," *Chemical Communications*, no. 39, pp. 5844–5846, 2009.

[30] P. Wang, S. M. Zakeeruddin, J. E. Moser, M. K. Nazeeruddin, T. Sekiguchi, and M. Grätzel, "A stable quasi-solid-state dye-sensitized solar cell with an amphiphilic ruthenium sensitizer and polymer gel electrolyte," *Nature Materials*, vol. 2, no. 6, pp. 402–407, 2003.

[31] M.-X. Li, H.-X. Zhang, X. Zhou, Q.-J. Pan, H.-G. Fu, and C.-C. Sun, "Theoretical studies of the electronic structure and spectroscopic properties of $[Ru(Htcterpy)(NCS)_3]^{3-}$," *European Journal of Inorganic Chemistry*, no. 15, pp. 2171–2180, 2007.

[32] D. Kuang, C. Klein, S. Ito et al., "High-Efficiency and stable mesoscopic dye-sensitized solar cells based on a high molar extinction coefficient ruthenium sensitizer and nonvolatile electrolyte," *Advanced Materials*, vol. 19, no. 8, pp. 1133–1137, 2007.